



University of Kentucky  
UKnowledge

---

Physics and Astronomy Faculty Publications

Physics and Astronomy

---

9-1-2012

# Improved He I Emissivities in the Case B Approximation

R. L. Porter  
*University of Georgia*

Gary J. Ferland  
*University of Kentucky, gary@uky.edu*

P. J. Storey  
*University College London, UK*

M. J. Detisch  
*University of Kentucky*

**Right click to open a feedback form in a new tab to let us know how this document benefits you.**

Follow this and additional works at: [https://uknowledge.uky.edu/physastron\\_facpub](https://uknowledge.uky.edu/physastron_facpub)

 Part of the [Astrophysics and Astronomy Commons](#), and the [Physics Commons](#)

---

## Repository Citation

Porter, R. L.; Ferland, Gary J.; Storey, P. J.; and Detisch, M. J., "Improved He I Emissivities in the Case B Approximation" (2012).  
*Physics and Astronomy Faculty Publications*. 242.  
[https://uknowledge.uky.edu/physastron\\_facpub/242](https://uknowledge.uky.edu/physastron_facpub/242)

This Article is brought to you for free and open access by the Physics and Astronomy at UKnowledge. It has been accepted for inclusion in Physics and Astronomy Faculty Publications by an authorized administrator of UKnowledge. For more information, please contact [UKnowledge@lsv.uky.edu](mailto:UKnowledge@lsv.uky.edu).

---

**Improved He I Emissivities in the Case B Approximation****Notes/Citation Information**

Published in *Monthly Notices Letters of the Royal Astronomical Society*, v. 425, no. 1, p. L28-L31.

This article has been accepted for publication in *Monthly Notices Letters of the Royal Astronomical Society* ©: 2012 The Authors. Published by Oxford University Press on behalf of the Royal Astronomical Society. All rights reserved.

**Digital Object Identifier (DOI)**

<http://dx.doi.org/10.1111/j.1745-3933.2012.01300.x>

# Improved He I emissivities in the case B approximation

R. L. Porter,<sup>1,2\*</sup> G. J. Ferland,<sup>3</sup> P. J. Storey<sup>4</sup> and M. J. Detisch<sup>3</sup>

<sup>1</sup>*Department of Physics and Astronomy, University of Georgia, Athens, GA 30602, USA*

<sup>2</sup>*Center for Simulational Physics, University of Georgia, Athens, GA 30602, USA*

<sup>3</sup>*Department of Physics & Astronomy, University of Kentucky, Lexington, KY 40506, USA*

<sup>4</sup>*Department of Physics & Astronomy, University College London, Gower Street, London WC1E 6BT*

Accepted 2012 June 2. Received 2012 June 1; in original form 2012 May 27

## ABSTRACT

We update our prior work on the case B collisional-recombination spectrum of He I to incorporate ab initio photoionization cross-sections. This large set of accurate, self-consistent cross-sections represents a significant improvement in He I emissivity calculations because it largely obviates the piecemeal nature that has marked all modern works. A second, more recent set of ab initio cross-sections is also available, but we show that those are less consistent with bound–bound transition probabilities than our adopted set. We compare our new effective recombination coefficients with our prior work and our new emissivities with those by other researchers, and we conclude with brief remarks on the effects of the present work on the He I error budget. Our calculations cover temperatures  $5000 \leq T_e \leq 25\,000$  K and densities  $10^1 \leq n_e \leq 10^{14}$  cm<sup>-3</sup>. Full results are available online (see Supporting Information).

**Key word:** atomic data.

## 1 INTRODUCTION

The high precision required to make a significant measurement of the primordial helium abundance presents challenges that are unique in nebular astrophysics. The recombination rate coefficients, needed to convert emission-line intensities into ionic abundance ratios, must have an accuracy better than the precision expected for the derived abundance. Usually we hope to measure abundances of most elements to an accuracy of 20–30 per cent. The primordial helium problem requires recombination rates accurate to better than a per cent, presenting unprecedented challenges to the atomic physics of the line formation. See Brocklehurst (1972) and references therein for early seminal work in the field of theoretical He I emissivities.

We need four types of atomic data to calculate the case B recombination spectrum: level energies, transition probabilities, photoionization cross-sections and collision rates. Porter et al. (2009) summarize the contributors to the error budget. Energy uncertainties have always been negligible compared to other sources, and accurate transition probabilities have been available since Kono & Hattori (1984). Drake (1996) and Drake & Morton (2007) improved upon the latter still further.

Photoionization cross-sections and collision rates represent the greatest sources of uncertainties in current standard calculations of He I emissivities (Benjamin, Skillman & Smits 1999, hereafter BSS99; Porter et al. 2005; Porter, Ferland & MacAdam 2007). For the low-density, extragalactic observations used in primordial helium analyses (Izotov, Thuan & Stasińska 2007; Peimbert, Luridiana

& Peimbert 2007; Aver, Olive & Skillman 2010), photoionization cross-sections (and, by extension, recombination coefficients) are the greatest source of uncertainty (Porter et al. 2009). See Ferland et al. (2010) for a recent review of the errors in He I emissivities and in primordial helium abundances.

In this Letter we update our earlier calculations of case B, He I emissivities (Bauman et al. 2005; Porter et al. 2005, 2007) to include a large set of self-consistent, ab initio photoionization cross-sections. We compare our present results with our previous work, with those by BSS99 and by Almog & Netzer (1989). We present here a subset of our present results that is most applicable to primordial helium research. A much larger set is available in the electronic edition.

## 2 ATOMIC DATA

The first large set ( $L \leq 4$  and  $n \leq 25$ ) of modern, self-consistent photoionization cross-sections was calculated by Hummer & Storey (1998, hereafter HS98). However, the full set has remained unpublished. Ercolano & Storey (2006) used the full set to produce accurate continuous emission spectra. The current work represents the first use in case B line emissivity calculations.

Another large set of photoionization cross-sections was presented recently by Nahar (2010). Because highly accurate bound–bound absorption oscillator strengths obtained with Hylleraas-type wavefunctions are available (Drake 1996), we can readily apply a simple extrapolation method (Burgess & Seaton 1960) to judge the accuracy of free–bound differential oscillator strengths at the ionization threshold. HS98 applied this method to several low-lying levels of

\*E-mail: ryanlporter@gmail.com

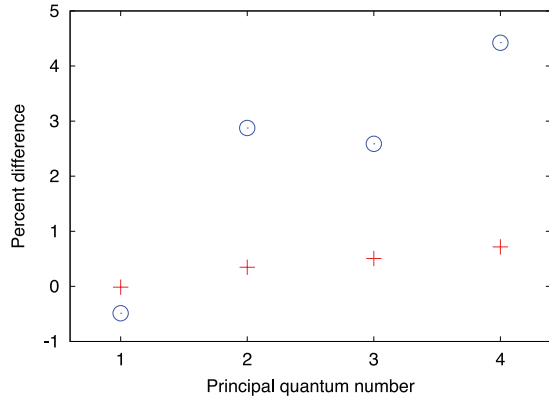


**Figure 1.** Percentage differences for threshold photoionization cross-sections of  $ns\ ^1S$  states relative to ‘extrapolated’ Drake (1996) results. Nahar (2010, blue circles), HS98 (red crosses).

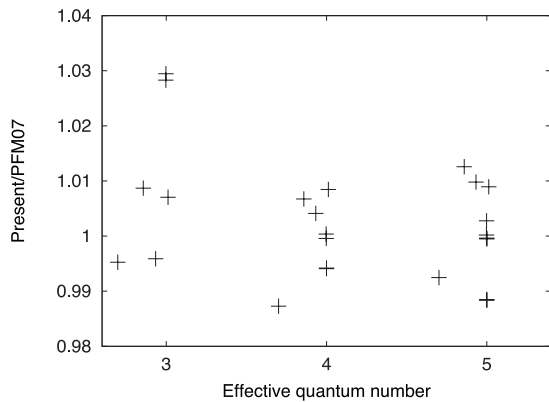


**Figure 2.** Ratio of present to PFM07 effective recombination coefficients in the low-density limit at 10 000 K. The three levels with the largest changes are  $3d\ ^1D$ ,  $3d\ ^3D$  and  $5s\ ^1S$  (see text). The differences will generally be smaller at finite densities.

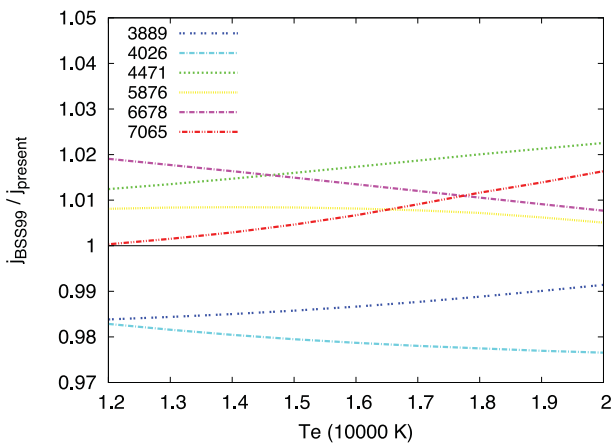


**Figure 3.** Ratio of BSS99 to present emissivities for several strong lines as a function of temperature with  $n_e = 100\text{ cm}^{-3}$ . This figure should be compared with fig. 5 of Aver et al. (2010). The principal effect is that for both  $\lambda\lambda 5876, 6678$ , the present results are greater than the earlier Porter et al. works and are roughly the average of the BSS99 results and our earlier work. Our  $\lambda\lambda 3889, 7065$  results have also changed considerably, and (within the plotted temperature range) the ratios no longer cross the ‘zero deviation line’ discussed by Aver et al. (2010).

**Table 1.** Wavelengths and upper and lower levels of reported lines.

Wavelength ( $\text{\AA}$ , air)	Upper level	Lower level
2945	$5p\ ^3P$	$2s\ ^3S$
3188	$4p\ ^3P$	$2s\ ^3S$
3614	$5p\ ^1P$	$2s\ ^1S$
3889	$3p\ ^3P$	$2s\ ^3S$
3965	$4p\ ^1P$	$2s\ ^1S$
4026	$5d\ ^3D$	$2p\ ^3P$
4121	$5s\ ^3S$	$2p\ ^3P$
4388	$5d\ ^1D$	$2p\ ^1P$
4438	$5s\ ^1S$	$2p\ ^1P$
4471	$4d\ ^3D$	$2p\ ^3P$
4713	$4s\ ^3S$	$2p\ ^3P$
4922	$4d\ ^1D$	$2p\ ^1P$
5016	$3p\ ^1P$	$2s\ ^1S$
5048	$4s\ ^1S$	$2p\ ^1P$
5876	$3d\ ^3D$	$2p\ ^3P$
6678	$3d\ ^1D$	$2p\ ^1P$
7065	$3s\ ^3S$	$2p\ ^3P$
7281	$3s\ ^1S$	$2p\ ^1P$
9464	$5p\ ^3P$	$3s\ ^3S$
10830	$2p\ ^3P$	$2s\ ^3S$
11013	$5p\ ^1P$	$3s\ ^1S$
11969	$5d\ ^3D$	$3p\ ^3P$
12527	$4p\ ^3P$	$3s\ ^3S$
12756	$5p\ ^1P$	$3d\ ^1D$
12785	$5f\ ^3F$	$3d\ ^3D$
12790	$5f\ ^1F$	$3d\ ^1D$
12846	$5s\ ^3S$	$3p\ ^3P$
12968	$5d\ ^1D$	$3p\ ^1P$
12985	$5p\ ^3P$	$3d\ ^3D$
13412	$5s\ ^1S$	$3p\ ^1P$
15084	$4p\ ^1P$	$3s\ ^1S$
17003	$4d\ ^3D$	$3p\ ^3P$
18556	$4p\ ^1P$	$3d\ ^1D$
18685	$4f\ ^3F$	$3d\ ^3D$
18697	$4f\ ^1F$	$3d\ ^1D$
19089	$4d\ ^1D$	$3p\ ^1P$
19543	$4p\ ^3P$	$3d\ ^3D$
20427	$6p\ ^3P$	$4s\ ^3S$
20581	$2p\ ^1P$	$2s\ ^1S$
20602	$7d\ ^3D$	$4p\ ^3P$
21118	$4s\ ^3S$	$3p\ ^3P$
21130	$4s\ ^1S$	$3p\ ^1P$
21608	$7f\ ^3F$	$4d\ ^3D$
21617	$7f\ ^1F$	$4d\ ^1D$

He I and tabulated results in their table 1. In Fig. 1, we compare those results with the ab initio calculations of  $ns\ ^1S$  levels from both Nahar and HS98. Nahar’s values disagree with the extrapolated cross-sections by as much as 4 per cent. The HS98 cross-sections are clearly more consistent with the Drake results than are the Nahar (2010) values. The target wavefunctions used in HS98 were derived from those of Calvert & Davison (1971) and were designed to fully represent the dipole and quadrupole polarizability of the  $\text{He}^+$  ground state and to include short-range correlation optimized on the energies of the  $ns\ ^1S$  states, which were known to be particularly difficult to represent. This target provides very accurate results at energies near threshold, as required for the temperature range and applications discussed here but is unsuitable at higher energies. The target used by Nahar (2010) is extensive and implicitly treats polarization and correlation effects, but it is not optimized for near-threshold calculation or for the  $ns\ ^1S$  states. It is, however, applicable over a much larger energy range than that used in HS98.

**Table 2.** Emissivities of several He I lines at conditions important for primordial abundance analyses. This table is a small subset of the full results. Values are  $4\pi j/n_e n_{\text{He}}$  in units of  $10^{-25} \text{ erg cm}^3 \text{ s}^{-1}$ .

$T_e$ (K)	$n_e$ ( $\text{cm}^{-3}$ )	3889 Å	4026 Å	4471 Å	5876 Å	6678 Å	7065 Å
10 000	10	1.3889	0.2902	0.6098	1.6782	0.4706	0.2875
11 000	10	1.2980	0.2652	0.5549	1.5112	0.4229	0.2727
12 000	10	1.2194	0.2440	0.5086	1.3721	0.3833	0.2600
13 000	10	1.1507	0.2257	0.4690	1.2546	0.3498	0.2487
14 000	10	1.0901	0.2098	0.4347	1.1542	0.3213	0.2388
15 000	10	1.0360	0.1959	0.4047	1.0674	0.2966	0.2299
16 000	10	0.9875	0.1835	0.3783	0.9917	0.2751	0.2218
17 000	10	0.9437	0.1726	0.3549	0.9252	0.2562	0.2145
18 000	10	0.9039	0.1627	0.3340	0.8663	0.2395	0.2078
19 000	10	0.8676	0.1539	0.3153	0.8138	0.2247	0.2017
20 000	10	0.8343	0.1459	0.2983	0.7668	0.2113	0.1960
10 000	100	1.3989	0.2904	0.6101	1.6768	0.4692	0.2975
11 000	100	1.3100	0.2655	0.5557	1.5138	0.4224	0.2848
12 000	100	1.2334	0.2444	0.5099	1.3787	0.3836	0.2738
13 000	100	1.1666	0.2263	0.4708	1.2650	0.3509	0.2642
14 000	100	1.1077	0.2105	0.4370	1.1682	0.3230	0.2557
15 000	100	1.0553	0.1968	0.4075	1.0848	0.2990	0.2480
16 000	100	1.0082	0.1846	0.3817	1.0123	0.2782	0.2409
17 000	100	0.9657	0.1738	0.3587	0.9487	0.2598	0.2345
18 000	100	0.9270	0.1641	0.3383	0.8926	0.2437	0.2285
19 000	100	0.8917	0.1554	0.3200	0.8428	0.2293	0.2231
20 000	100	0.8592	0.1475	0.3036	0.7984	0.2164	0.2181
10 000	1000	1.4701	0.2928	0.6175	1.7310	0.4780	0.3754
11 000	1000	1.3969	0.2687	0.5661	1.5893	0.4350	0.3771
12 000	1000	1.3353	0.2486	0.5235	1.4761	0.4000	0.3790
13 000	1000	1.2823	0.2315	0.4877	1.3842	0.3712	0.3807
14 000	1000	1.2359	0.2168	0.4574	1.3084	0.3470	0.3816
15 000	1000	1.1945	0.2040	0.4313	1.2449	0.3266	0.3818
16 000	1000	1.1571	0.1929	0.4087	1.1910	0.3090	0.3811
17 000	1000	1.1227	0.1830	0.3888	1.1444	0.2937	0.3797
18 000	1000	1.0910	0.1743	0.3714	1.1041	0.2803	0.3778
19 000	1000	1.0618	0.1666	0.3561	1.0706	0.2683	0.3765
20 000	1000	1.0344	0.1596	0.3424	1.0408	0.2577	0.3746

We use the unpublished cross-sections described by HS98. For  $n \leq 4$  and  $L \leq 2$ , we rescale to agree at threshold to those extrapolated from the Drake oscillator strengths and listed in table 1 of HS98. We use the extrapolation procedure described by HS98 to obtain values for  $n = 5$  and  $L \leq 2$ , but these normalizations have only minor effects on the emissivities of the most important lines.

We follow HS98 and assume that recombination coefficients are fixed relative to hydrogen for  $n > 25$  and  $L \leq 2$ . All other aspects of our calculations are as described in Bauman et al. (2005). Briefly, this entails  $nLS$ -resolved levels for  $n \leq 100$ , a single ‘collapsed’ level at  $n = 101$  and collisions induced by electrons, protons and  $\text{He}^+$ . The calculations are performed with a development version of the spectral simulation code CLOUDY (last described by Ferland et al. 1998).<sup>1</sup>

Following Switzer & Hirata (2008), we also have added radiative bound–bound electric quadrupole transitions (Cann & Thakkar 2002). However, these transitions have a negligible effect on the present results; we mention the change for completeness and to note that these transitions may be important for high- $Z$  He-like ions (as in Porter & Ferland 2007).

<sup>1</sup> The  $J$ -resolved code described by Bauman et al. (2005) has also been updated with the HS98 cross-sections. That code can be retrieved with a subversion client from <https://svn.nublado.org/bauman/source>.

Finally, we note that we have compared our existing implementation of heavy particle angular momentum changing collisions to the new results by Vrinceanu, Onofrio & Sadehpour (2012) and found excellent agreement.

### 3 RESULTS AND DISCUSSION

We compare effective recombination coefficients in our new treatment with those of Porter et al. (2007) in Fig. 2. For the majority of levels the change is  $\lesssim 1$  per cent. There are two clear exceptions, corresponding to  $3d^1D$  and  $3d^3D$ . The cause is a programming error in our earlier renormalization of the Peach (1967) cross-sections. There are only two levels affected. Unfortunately, these are the upper levels of two of the most important lines in primordial helium abundance works:  $\lambda\lambda 5876, 6678$ . The new results yield stronger emissivities for both lines. The next largest differences in Fig. 2 correspond to levels with only weak optical lines.

We compare our new emissivities with BSS99 for several strong lines in Fig. 3. This figure is directly comparable to fig. 5 of Aver et al. (2010). Consistent with the discussion above,  $j_{5876}$  and  $j_{6678}$  are now in better agreement with BSS99, though important differences clearly remain.

Our calculations cover  $5000 \leq T \leq 25\,000$  K (in 1000-K steps) and  $10^1 \leq n_e \leq 10^{14} \text{ cm}^{-3}$  (in 1-dex steps). In addition to the

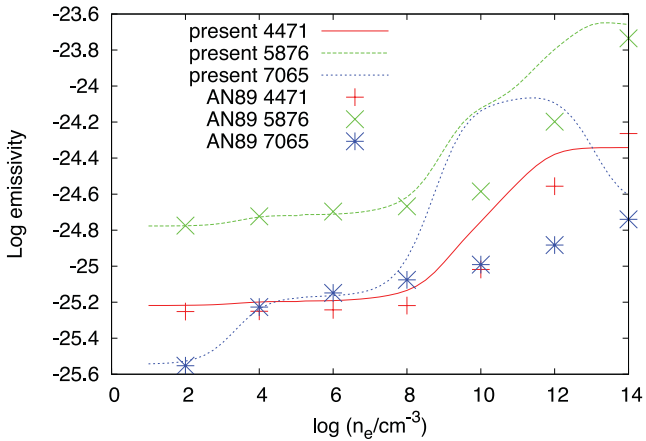


**Figure 4.** Comparison of present emissivity calculations to those by AN89 as a function of density at 10000 K.

lines published in our prior work, we have also included several weak infrared lines. Table 1 lists the wavelength and upper and lower level designations of all reported lines. Table 2 contains a small subset of the full results that is most applicable to primordial helium abundance calculations.

Almog & Netzer (1989, hereafter AN89) also presented He I emissivities for electron densities up to  $10^{14} \text{ cm}^{-3}$ . In Fig. 4 we compare present emissivities in  $\lambda\lambda 4471, 5876, 7065$  to the AN89 results (with  $\tau_{3889} = 0$ ). The calculations generally agree for  $n_e \lesssim 10^8 \text{ cm}^{-3}$  (where collisions do not dominate over radiative processes) and for  $n_e \sim 10^{14} \text{ cm}^{-3}$  (where collisions are so dominant that levels are approaching local thermodynamic equilibrium). Critical densities for levels with  $n \sim 3$  or 4 fall between these regions. Collisions are dominated by excitations from the metastable  $2s \ ^3S$ , which is treated in both the present work and AN89. Our work clearly has enhanced collisional excitation relative to AN89, and differences between the two calculations are strongly correlated with the relative collisional contributions given in table 5 of Porter et al. (2007). Note, however, that those collisional contributions should not be added to the present tabulations; they are already included.

A recalculation of the Monte Carlo error analyses performed in Porter et al. (2009) is beyond the scope of this Letter. We expect that our analysis of the relatively high density ‘Galactic’ model would be largely unchanged, as collisional uncertainties should dominate both before and after the present work. In the low-density ‘extragalactic’ model, however, our ‘optimistic’ uncertainties now seem somewhat more *realistic*. Total uncertainties are largely due to uncertainties in threshold photoionization cross-sections. One measure of those uncertainties (used by Porter et al. 2009) is the difference ( $\lesssim 0.7$  per cent) between the extrapolated threshold cross-sections and the HS98 ab initio results. Goodness of the fits used to extrapolate threshold cross-sections, including sensitivity of the fits to the number of terms used in the fitting procedure, is another measure, and we obtain  $\lesssim 0.2$  per cent for all levels with  $n \leq 5$ .

## ACKNOWLEDGMENTS

RLP thanks Leticia Martın Hernandez for the suggestion to publish results for several of the weaker  $\sim 2 \mu\text{m}$  lines (included in the full

table), Keith MacAdam for helpful comments and the referee for a valuable and practical suggestion. The authors thank the University of Kentucky Center of Computational Sciences for a generous allotment of computer time. GJF acknowledges support by NSF (0908877, 1108928 and 1109061), NASA (07-ATFP07-0124, 10-ATP10-0053 and 10-ADAP10-0073), JPL (RSA no. 1430426) and STScI (HST-AR-12125.01, GO-12560 and HST-GO-12309).

## REFERENCES

- Almog Y., Netzer H., 1989, MNRAS, 238, 57 (AN89)  
Aver E., Olive K. A., Skillman E. D., 2010, J. Cosmol. Astropart. Phys., 3, 1  
Bauman R. P., Porter R. L., Ferland G. J., MacAdam K. B., 2005, ApJ, 628, 541  
Benjamin R. A., Skillman E. D., Smits D. P., 1999, ApJ, 514, 307 (BSS99)  
Brocklehurst M., 1972, MNRAS, 157, 211  
Burgess A., Seaton M. J., 1960, MNRAS, 120, 121  
Calvert J. M., Davison W. D., 1971, J. Phys. B, 4, 314  
Cann N. M., Thakkar A. J., 2002, J. Phys. B, 35, 421  
Drake G. W. F., 1996, in Drake G. W., ed., Atomic, Molecular, and Optical Physics Handbook. AIP, Woodbury, p. 154  
Drake G. W. F., Morton D., 2007, ApJS, 170, 251  
Ercolano B., Storey P. J., 2006, MNRAS, 372, 1875  
Ferland G. J., Korista K. T., Verner D. A., Ferguson J. W., Kingdon J. B., Verner E. M., 1998, PASP, 110, 761  
Ferland G. J., Izotov Y., Peimbert A., Peimbert M., Porter R. L., Skillman E., Steigman G., 2010, Proc. IAU Symp. 268, Light Elements in the Universe. Cambridge Univ. Press, Cambridge, p. 163  
Hummer D. G., Storey P. J., 1998, MNRAS, 297, 1073 (HS98)  
Izotov Y. I., Thuan T. X., Stasinska G., 2007, ApJ, 662, 15  
Kono A., Hattori S., 1984, Phys. Rev. A, 29, 2981  
Nahar S., 2010, New Astron., 15, 5  
Peach G., 1967, Mem. R. Astron. Soc., 71, 13  
Peimbert M., Luridiana V., Peimbert A., 2007, ApJ, 666, 636  
Porter R. L., Ferland G. J., 2007, ApJ, 664, 586  
Porter R. L., Bauman R. P., Ferland G. J., MacAdam K. B., 2005, ApJ, 622, L73  
Porter R. L., Ferland G. J., MacAdam K. B., 2007, ApJ, 657, 327  
Porter R. L., Ferland G. J., MacAdam K. B., Storey P. J., 2009, MNRAS, 393, 36  
Switzer E. R., Hirata C. M., 2008, Phys. Rev. D, 77, 083006  
Vrinceanu D., Onofrio R., Sadeghpour H. R., 2012, ApJ, 747, 56

## SUPPORTING INFORMATION

Additional Supporting Information may be found in the online version of this article.

**Table.** Calculated He I emissivities in the Case B approximation as a function of temperature and electron density. Details are included at the beginning of the uncompressed file.

Please note: Wiley-Blackwell are not responsible for the content or functionality of any supporting materials supplied by the authors. Any queries (other than missing material) should be directed to the corresponding author for the article.

This paper has been typeset from a  $\text{\TeX}/\text{\LaTeX}$  file prepared by the author.